Geomechanics and Engineering, *Vol. 24, No. 4 (2021) 359-370*
DOI: https://doi.org/10.12989/gae.2021.24.4.359

Geostatistical algorithm for evaluation of primary and secondary roughness

Hojat Nasab[1a], Saeed Karimi-Nasab*[1] and Hossein Jalalifar[2b]

[1]*Department of Mining Engineering, Shahid Bahonar University of Kerman, 76196-37147 Kerman, Iran*
[2]*Department of Oil Engineering, Shahid Bahonar University of Kerman, Kerman, Iran*

(Received September 13, 2020, Revised January 25, 2021, Accepted January 29, 2021)

Abstract. Joint roughness is combination of primary and secondary roughness. Ordinarily primary roughness is a geostatistical part of a joint surface that has a periodic nature but secondary roughness or unevenness is a statistical part of that which have a random nature. Using roughness generating algorithms is a useful method for evaluation of joint roughness. In this paper after determining geostatistical parameters of the joint profile, were presented two roughness generating algorithms using Mount-Carlo method for evaluation of primary ($GJRGA_P$) and secondary ($GJRGA_S$) roughness. These based on geostatistical parameters (range and sill) and statistical parameters (standard deviation of asperities height, SD_H, and standard deviation of asperities angle, SD_A) for generation two-dimensional joint roughness profiles. In this study different geostatistical regions were defined depending on the range and SD_H. As SD_H increases, the height of the generated asperities increases and asperities become sharper and at a specific range (a specific curve) relation between SD_H and SD_A is linear. As the range in $GJRGA_P$ becomes larger (the base of the asperities) the shape of asperities becomes flatter. The results illustrate that joint profiles have larger SD_A with increase of SD_H and decrease of range. Consequencely increase of SD_A leads to joint roughness parameters such Z_2, Z_3 and R_p increases. The results showed that secondary roughness or unevenness has a great influence on roughness values. In general, it can be concluded that the shape and size of asperities are appropriate parameters to approach the field scale from the laboratory scale.

Keywords: joint roughness; classification; geostatistical method; generation algorithm; JRC

1. Introduction

Sample selection is the primary objective in any parametric study in rock mechanics. Interpretation of the shear stress versus shear displacement curve of direct shear tests on natural rock joints is complicated due to joint roughness variability (Atapour and Moosavi (2014)). In order to evaluate the effect of joint roughness on shear behavior a variety of samples are used. These include two main groups. In the first group, shear strength models using artificial and natural material (artificial samples) are developed (usually a mixture of plaster or cement with other materials). In the second group, natural samples with pre-existing crack or natural samples with crack created in laboratory using Brazilian test or sawing machines are used (Atapour and Moosavi (2014)). Natural and artificial joint samples generally include: Natural samples with pre-existing crack (NPC), natural samples with the crack created in laboratory (NCC), artificial crack with remolded crack on natural crack (ARC), artificial samples with specific geometry of crack (ASC) and artificial samples with specific geometry of crack generated with a specific algorithm (ASA). Fig. 1 illustrates some types of joint surface for evaluation of joint roughness.

Joint roughness is one of the effective parameters in mechanical and hydro-mechanical behavior of rock mass, Wittke (2014). Joint roughness is divided into small scale roughness or unevenness and large scale roughness or waviness, Mechanics (1978). Researchers have encountered serious challenges due to existence of unevenness and limitation of sampling dimension in laboratory scale. A lot of methods such as experimental, statistical and fractal methods have been suggested for evaluation of joint roughness (Barton and Choubey (1977), Mechanics (1978), Babanouri *et al.* (2013), Park *et al.* (2013), Babanouri and Karimi-Nasab 2015, Fathi *et al.* (2016) and Zhao *et al.* (2018)). For many decades quantification of experimental Barton profiles has been an interesting area of study by researchers. Many parameters have been defined for quantification of roughness (Grasselli (2001)) (e.g., Z_2 ،Z_3 ، Z_4 and Rp defined in Table 1). In quantitative description of joint roughness the asperities angle is quite effective. The Z_2 ،Z_3 ،Z_4 parameters are dependent to the angle of asperities. Z_2 is defined as the average of asperity angles. Z_3 illustrates curvature of asperities and Z_4 illustrates difference of projected positive and negative asperities, Gravanis and Pantelidis (2019). Asadi and Rasouli (2010) discuss that when the average of asperity angle is zero, standard deviation of asperity angles (SD_A) is a good criterion for definition of joint roughness, Asperity angle is related to the vertical and horizontal differential of two points at a joint roughness profile. Joint roughness is a

∗Corresponding author, Associate Professor
E-mail: kariminasab@uk.ac.ir
[a]Ph.D. Student
E-mail: nasab.hojat@gmail.com
[b]Professor
E-mail: jalalifar@uk.ac.ir

ISSN: 2005-307X (Print), 2092-6219 (Online)

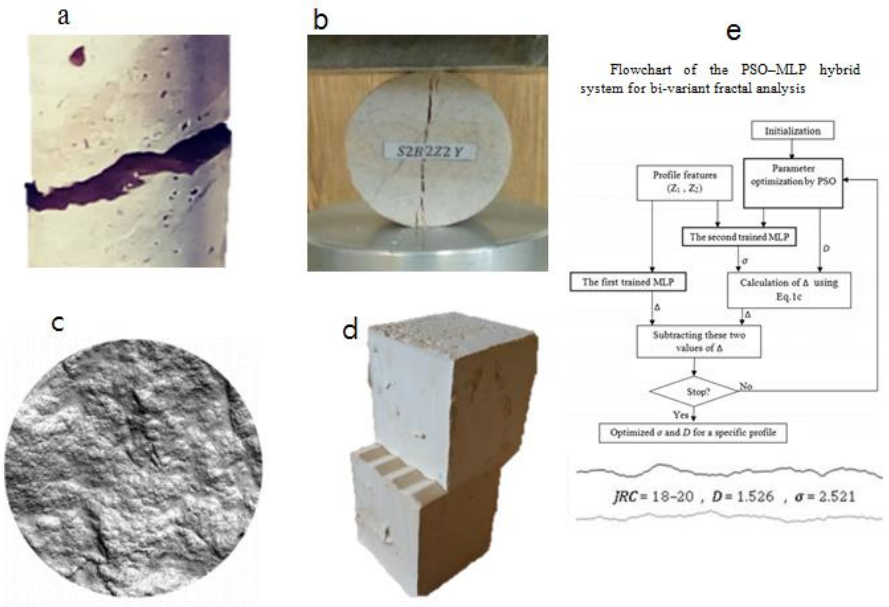

Fig. 1 Different types of surface for evaluation of joint roughness (a) Natural samples with pre-existing crack (NPC), (b) Natural samples with the crack created in laboratory (NCC), (c) Artificial crack with remolded crack on natural crack (ARC) Babanouri and Karimi-Nasab (2015), (d) Triangle roughness (ASC) and (e) Artificial samples with specific geometry of crack generated with a specific algorithm (ASA) Babanouri *et al.* (2013)

Table 1 Statistical parameters for joint roughness description Parameters

Parameters	
$Z_2 = \left[\frac{1}{M(D_x)^2}\sum_{i=1}^{M}(Z_{i+1}-Z_i)^2\right]^{0.5}$ and $Dx = x_{i+1} - x_i$	Z_2: average of asperities angles Gravanis and Pantelidis (2019)
$Z_3 = \frac{1}{L}\sqrt{\int_{x=0}^{x=L}\left(\frac{d^2y}{dx^2}\right)^2 dx}$	Z_3: curvature of asperities, Gravanis and Pantelidis (2019)
$Z_4 = \frac{\sum_{i=1}^{N} x_{i+} - \sum_{i=1}^{N} x_{i-}}{L}$	Z_4: relation between difference of projected positive and negative asperities to the length of profile, Gravanis and Pantelidis (2019)
$R_p = \frac{[\sum_{i=1}^{n-1}[(Z_{i+1}-Z_i)^2 + (x_{i+1}-x_i)^2]^{0.5}}{L}$	R_p: relation between actual to projected joint roughness profile, Grasselli (2001)

Table 2 Geostatistical models for defining joint roughness

Parameter: a=Range, C=Sill and e= the base of the Natural (Neper)	Model	Reference
$SR_v = \frac{\sqrt{2C}}{a}$, $SR_v \in (0,\infty)$	$JRC = 7.158\ln(SR_v) + 31.218$	Chen *et al.* (2016)
$CA = \sqrt{\frac{2}{e}}.\frac{C}{a}$	$JRC = 33.06(CA)^{0.1593} + 9.475$	Zhao *et al.* (2018)

geostatistical parameter.

Geostatistical approach is another method for evaluation of joint surfaces. Geostatistical method is mainly based on the variation of asperities height related to the lag distance. Height of asperities is usually the regional variable to evaluate joint surface (Fecker (1978)). One of the most important advantage of the method is determination of free scale shear strength model. Fecker (1978), determined variogram of Barton profile at 0.33 cm interval sampling. Chen *et al.* (2016) suggested SRv index as geostatistical parameters for determination of joint roughness Zhao *et al.* (2018) with evaluation of different variogram models, were defined CA index for determination of joint roughness. These two models are given in Table 2.

These equations show that the asperities height is not a statistical quantity and consider it as a geostatistical

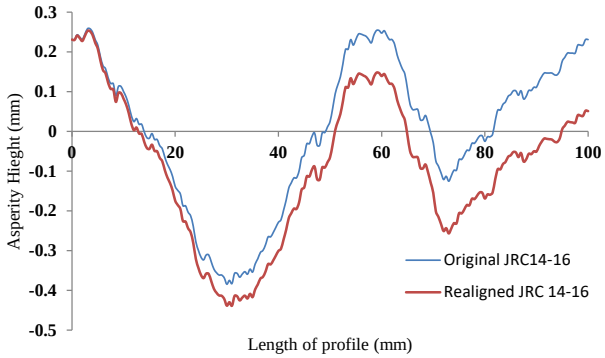

Fig. 2 Original and realigned profile of Barton (JRC 14-16)

Table 3 The first three probability density function (PDF) of asperities height

JRC	Rank 1	Rank 2	Rank 3
OR-JRC 2-4	Dagum (4P)	Kumaraswamy	Beta
Re-JRC 2-4	Dagum (4P)	Kumaraswamy	Beta
OR-JRC4-6	Gen. Extreme Value	Wakeby	Dagum (4P)
Re-JRC 4-6	Wakeby	Gen. Extreme Value	Gamma (3P)
OR-JRC6-8	Frechet (3P)	Triangular	Gamma (3P)
Re-JRC 6-8	Wakeby	Johnson SB	Gen. Extreme Value
OR-JRC8-10	Wakeby	Gen. Extreme Value	Johnson SB
Re-JRC 8 -10	Log-Logistic (3P)	Dagum (4P)	Fatigue Life (3P)
OR-JRC10-12	Wakeby	Gen. Pareto	Uniform
Re-JRC 10-12	Beta	Power Function	Wakeby
OR-JRC12-14	Error	Gen. Gamma (4P)	Gen. Extreme Value
Re-JRC 12-14	Dagum (4P)	Johnson SB	Beta
OR-JRC14-16	Wakeby	Johnson SB	Gen. Extreme Value
Re-JRC 14-16	Wakeby	Gen. Extreme Value	Johnson SB
OR-JRC16-18	Beta	Kumaraswamy	Error
Re-JRC 16-18	Johnson SB	Beta	Kumaraswamy
OR-JRC18-20	Beta	Kumaraswamy	Johnson SB
Re-JRC-18-20	Wakeby	Dagum (4P)	Gen. Logistic

quantity. The most common method for evaluation of joint roughness is using standard profiles of Barton and Chouby (Barton and Choubey (1977)). These profiles are the basic of most studies performed to quantify of joint roughness. However in reality there are many rock joint surfaces that have different morphology but have a same roughness value (Grasselli and Egger (2003), Babanouri *et al.* (2013), Huan *et al.* (2019), Lotfi and Tokhmechi (2019), Yong, *et al.* (2019)). Using an artificial profile with a specific geometry is one way to reduce the uncertainty of studies on joint roughness (He *et al.* (2014)).

There are a few methods for joint roughness profile generation. The Brownian algorithm based on the self-affine geometry is the most common method for joint roughness generation (Kulatilake *et al.* (1998)). Babanori *et al.* (2013) by using a complex algorithm found the best Brownian self-affine parameters for ten standard profiles of Braton. Hoàng Khanh Lê *et al.* (2018) determined variogram of profile height variation (PHV) for many joint roughness profiles. They found PHV is independent of spatial location. They assumed that PHV is a statistical parameter and they generated two dimensional joint roughness profiles by Monte Carlo method. They found that PHV joint roughness profiles have a normal probability distribution function (NPDF) with zero mean. They illustrated that with increase of standard deviation of PHV the joint roughness coefficient (JRC) also increased (Lê *et al.* 2018). The generated points from this algorithm are fixed at 0.25 mm distance from each other. The selection of the constant distance has a significant effect on JRC value. In this study, a new algorithm is suggested to use geostatistical parameters for generation of two dimensional roughness profiles. Subsequently, using generated profiles, joint roughness was evaluated.

2. Height probability distribution function of Barton profiles

The ten Barton and Chouby (original profiles) are

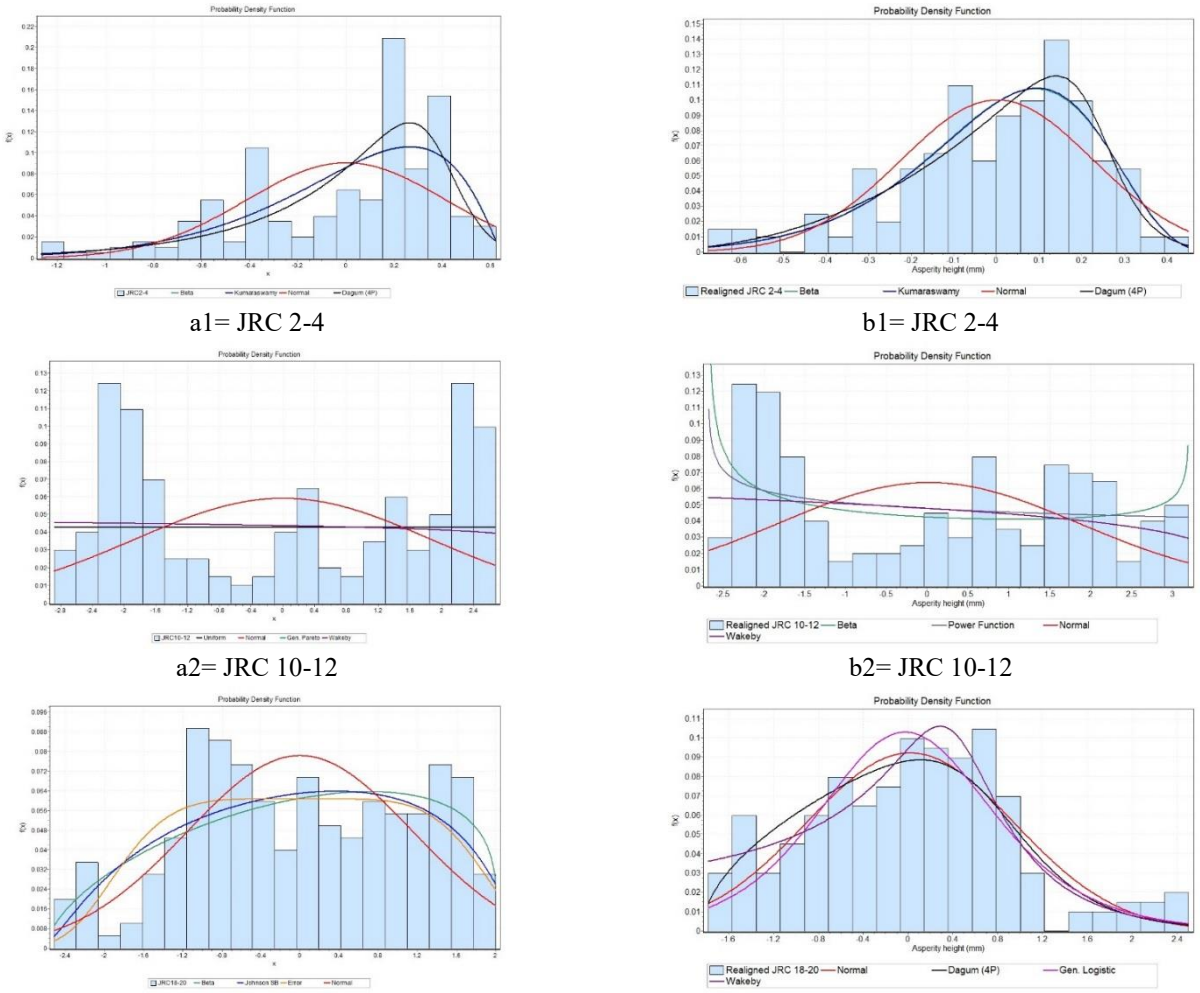

a1= JRC 2-4 b1= JRC 2-4

a2= JRC 10-12 b2= JRC 10-12

a3= JRC 18-20 b3= JRC 18-20

Fig. 3 Probability density function for original profiles (left) and realigned profiles (right)

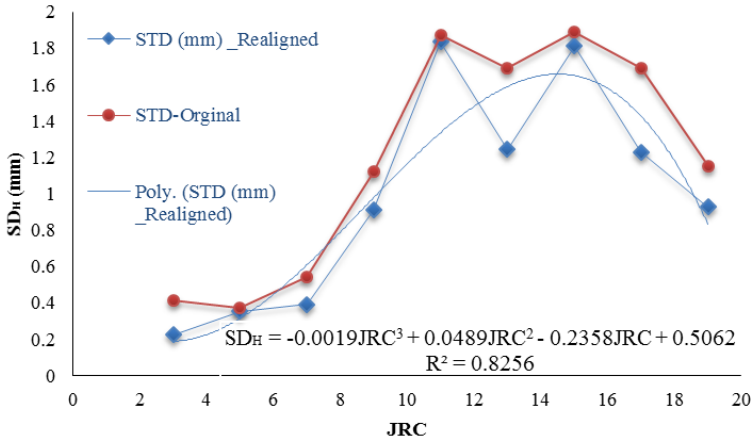

Fig. 4 Correlation between standard deviation of asperities height (SD_H) and JRC

obtained by the Profilometer with accuracy of about 1 mm. Some researchers have worked on the effect of sampling interval on the joint roughness (Tatone and Grasselli (2010)). Here an asperity height measurement with 0.5 mm interval scanning line is used. Tatone and Grasselli (2010) following digitization of the profiles noted that the original JRC profiles were not aligned so they re-aligned the original profiles (re-aligned profiles). The original and re-aligned profile of Barton (JRC 14-16) are shown in Fig. 2.

As mentioned before, a sampling interval of 0.5 mm was selected to extract data from the original profiles. To measure the asperity height a horizontal regression line with the minimum sum square of error (SSE) was selected. After measuring the height of joint roughness profiles,

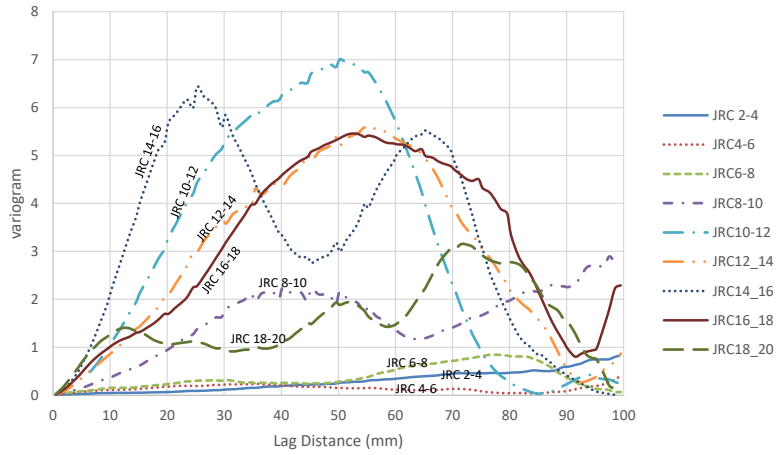

Fig. 5 Variogram of original profiles of Barton

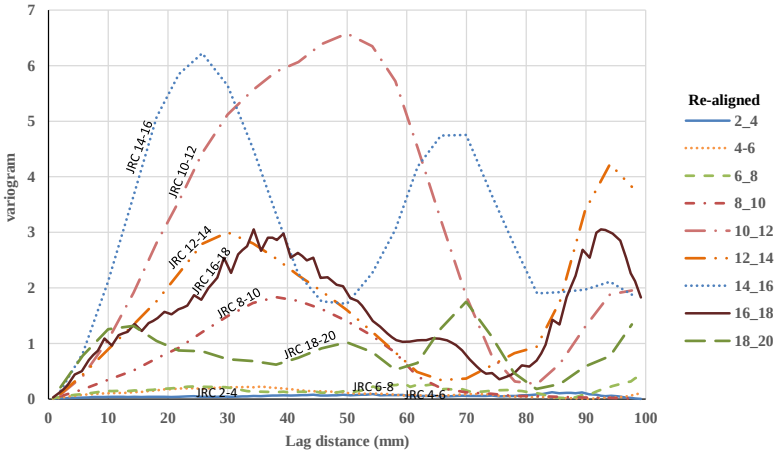

Fig. 6 Variogram of re-aligned profiles of Barton

probability density function (PDF) of joint roughness was determined. Then, the histogram of Barton profiles was determined. The asperities heights for JRC 2-4 (JRC 3), JRC 10-12 (JRC 11) and 20-18 (JRC 19) for original and realigned profiles are shown in Fig. 3. The three first asperities heights with normal PDF were computed based on Anderson-Darling method. The results are illustrated in Fig. 4. The left (a1, a2 and a3) and the right (b1, b2 and b3) side histograms belong to the original and re-aligned profiles of Barton respectively. Comparison of PDFs between original and realigned profiles illustrates that a small rotation of profiles can change the best fit of PDF. The best adjusted PDFs were not similar for different profiles. Table 3 illustrates the three first PDF of asperities heights for original profile (OR-JRC) and realigned profile (RE-JRC).

The various PDF definitions have been explained in the hand-book on statistical distributions for experimentalists (Walck (1996)). Due to large changes in PDFs, using PDF of asperities height is not a suitable method for description of joint roughness but the results illustrate that normal PDF is suitable for all Barton profiles. The normal (or Gaussian) distribution is a very common continuous probability distribution function. Normal distributions are important in statistics and are often used in the natural and social sciences to represent real-valued random variables whose distributions are not known. In this paper, normal distributions of original and realigned profiles are compared. Normal distribution is defined with mean and standard deviation (SD). Since a line with minimum sum square error (SSE) was selected for total trend of joint roughness the mean of asperities height is zero or near zero (below the 100 micrometer). Therefore, the standard deviation of asperities height (SD_H) of original and realigned profiles are compared. Correlation between SD_H and JRC is shown in Fig. 4.

Maximum change in SD_H (about 0.5 mm) for either original or re-aligned profiles occurs in JRC 13 and 17 for which the required rotation is about +1.93 and +2.1 degrees respectively. SD_H for all realigned profiles compared to original profiles is reduced. SD_H of asperity height is expected to increase but after JRC 11 the trend is changed and with increase of JRC, SD_H is reduced. SD_H is defined in Eq. (1) as a function of JRC. It is a three-order polynomial equation with root mean square equal to 0.82. Variation of SD_H and JRC are not proportional, hence, SD_H is not a suitable parameter for evaluation of joint roughness. Some of these mismatches are based on neglecting the role of the geostatistical parameters (radius effect (range), sill) asperities height on joint roughness coefficient.

$$SD_H = -0.0019JRC^3 + 0.0489JRC^2 - 0.2358JRC + 0.5062 \quad (1)$$

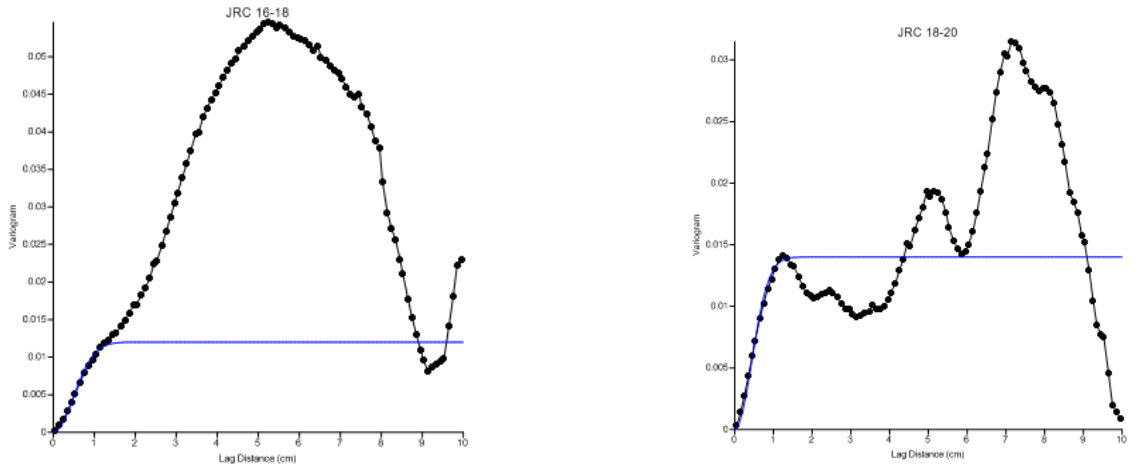

(a) JRC 16-18 (b) JRC 18-20

Fig. 7 Engineering judgment at determination of variogram models

Table 4 Geostatistical parameters for original and realigned profiles of Barton

JRC		2-4	4-6	6-8	8-10	10-12	12-14	14-16	16-18	18-20
JRC average		3	5	7	9	11	13	15	17	19
Original JRC	SD_H (mm)	0.42	0.37	0.54	1.12	1.87	1.69	1.89	1.69	1.15
	Sill (mm^2)	0.05	0.23	0.30	2.20	7.00	5.50	6.20	1.20	1.40
	Range (mm)	50.87	35.00	31.00	24.00	26.00	29.00	14.00	7.00	7.00
Realigned JRC	SD_H (mm)	0.22	0.35	0.39	0.91	1.84	1.24	1.81	1.23	0.93
	Sill (mm^2)	0.07	0.22	0.21	1.80	6.55	3.32	6.13	2.52	1.39
	Range (mm)	55.63	30.00	24.43	23.72	25.12	19.86	14.41	18.46	6.41

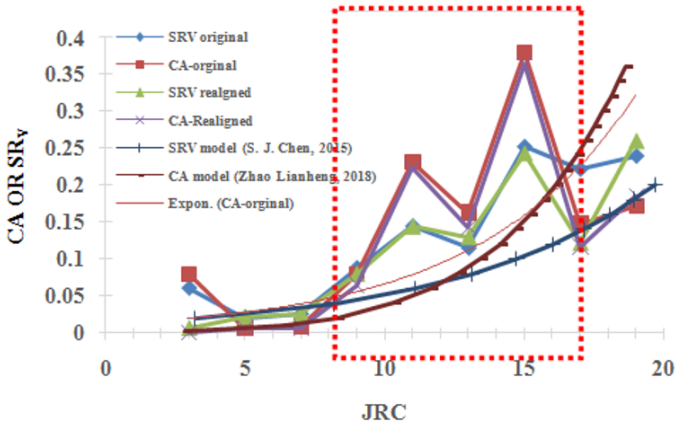

Fig. 8 Relation between CA / SRV and JRC

3. Geostatistical properties of Barton profiles

The first step of a geostatistical analysis is to identify the spatial structure of a regionalized variable (Fecker (1978)), which is the asperity height in this study. The geostatistical tool for joint roughness profile is the variogram. The spatial continuity and variability of fracture surfaces are described using the variogram (originally named as semivariogram). The semivariogram was first defined by Matheron (1963) as half the average squared difference between points z(x+h) and z(x) separated at distance h. The value of a variogram for the lag vector of h is defined as follows Eq. (2). In the variogram method, sill is the maximum variance of the asperities height, while range is a lag distance where the variance of regionalized variable approaches a constant value.

$$\gamma(h) = \frac{1}{2N(h)} \sum_{1}^{N(h)} [z(x+h) - z(x)]^2 \quad (2)$$

The wave form of a variogram shows a hole effect, which is typical of a periodic increment and decrement of regionalized variable. The obtained variogram for original and realigned JRC profiles are reported in Figs. 5 and 6

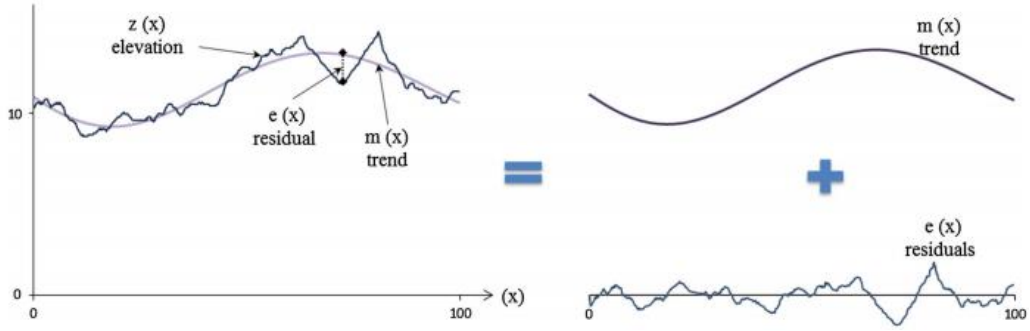

Fig. 9 Decomposition of spatial variation into primary and secondary roughness (Babanouri and Nasab 2015)

respectively. At the same profile length (here 100 mm), if the lag distance is increased, the number of pair points for determining variogram is reduced and thus the accuracy of variogram is reduced. Variogram of Original profiles of Barton has a trend, i.e. a gradual change in some property of the series over the whole interval under investigation. Realigned profile doesn't have a linear trend but an unknown trend appears after sill limit.

Post variation of variogram shows a semi-periodic behavior of asperity height. Therefore some methods, such as fractal method that are dependent to periodic phenomena have complexity and difficulties in the laboratory scale (Grasselli (2001)). A large range with a low sill indicates a smooth planar interface, while a large range with a large sill indicates a smooth undulating structure (Zhao *et al.* (2018)). In this respect, both the sill and range of the variogram are related to the joint roughness profile. Due to the trend of data, determination of exact amount of sill and range parameters for standard profiles of Barton is not possible and depends on engineering judgment. For example variograms of JRC 16-18 (JRC 17) and JRC 18-20 (JRC 19) are illustrated in Fig. 7. The general shape of the variogram is quite different, but the models fitted to the two variogram have the same range with different sill. In this study a point at variogram where the slope of the curve is changing was considered for the best fitted variogram model. Table 2 illustrates geostatistical properties of ten original and Re-aligned profiles of Barton.

The limit variation of the range of asperities height at Barton profiles is between 7-50.87 mm and the limit variation of the SD_H is between 0.39-1.89 mm. The calculated values of CA and SRv for realigned profiles are lower than the values for the original profiles. In the part determined by red dashed rectangle, waviness has the most effect on the results (Zhao *et al.* (2018)). The results show that the obtained range and sill have a good fitness with CA and SRv parameters. Coefficient of Determination (R^2) of CA relative to SRv is larger. It is interesting to note the difference in the presented models. This can be derived from different engineering judgment. In order to evaluate the results (Table 2) the CA and SRv parameters were calculated and the results are illustrated in Fig. 8.

4. Geostatistical joint roughness generation algorithm (GJRGA)

Jing *et al.* (1992) proposed a concept of primary and secondary roughness to explain the mechanical behaviors of rock fractures under shearing: the primary roughness (at large-scale is defined waviness) was defined as the dominating and larger-scale wavy surface undulation while the secondary roughness was defined as the randomly distributed small-scale unevenness that superimposed on the primary or waviness surfaces (Wang *et al.* (2016)). Fig. 9 illustrates decomposition of joint roughness profiles. Existence of unevenness and limitation of sample dimension (scale effect) is challenging for geotechnical researches.

The asperity angle is an effective parameter in definition of some joint roughness parameters such as Z_2, Z_3 and Z_4, but these parameters do not consider the shape effect of asperity on the roughness. The effect of asperity shape is shown in Fig. 10. The base and height of an asperity is defined by Δx and Δh respectively. Any changes to the ratio of Δh to Δx (asperity geometry) leads changes in the shape of asperity and it varies the roughness profile. Increasing the ratio of Δh to Δx induces a steep and sharper asperity, conversely decreasing the ratio of Δh to Δx induces a smooth asperity. Also the scale effect is shown in Fig. 10.

The shape of natural surface asperities of rough joint surfaces vary in size and shape (Fig.1(a)), which is described based on asperity geometry, therefore the ratio of Δh to Δx is various which leads to the variation of asperity angles. Variation of asperities height could be defined by SD_H, but joint roughness asperities with the same SD_H and different asperities base, have different asperity angles. So the bases of asperities have an important effect on the shape of joint asperity. As mentioned before, the maximum distance that asperities height correlates each other is defined as range, which is determined by variograms, as they could evaluate the spatial correlation of asperities height.

In this paper for evaluation of asperity height and asperity angle instead of Δh and asperity angle, SD_H and SD_A are used respectively. When the SD_H of the asperities is increased, the joint roughness is expected to be increased but as it is illustrated in Fig. 4 this relation is not always proportional and could be related to other parameters. Often asperity with larger range has a bigger size. Consequently range and SD_H have important effects on asperity angle so this study evaluates the interaction of these two parameters on SD_A.

One of the useful approaches for evaluation of different joint roughness profiles is using joint roughness generation

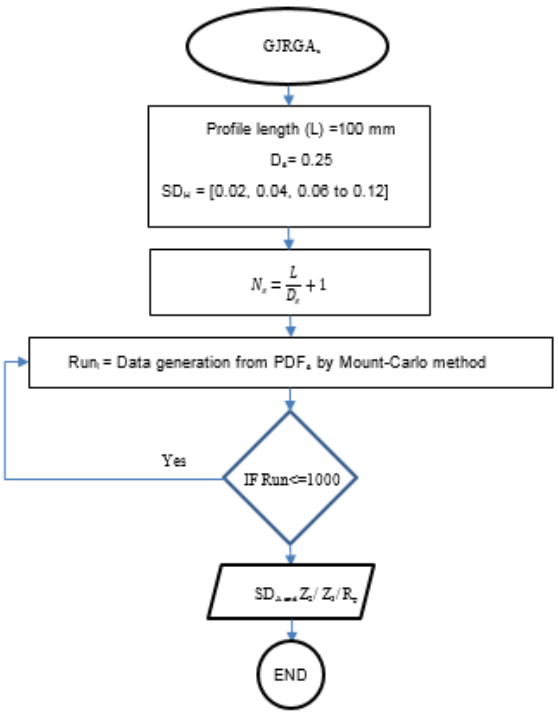

Fig. 11 Geostatistical joint roughness generation algorithm for secondary roughness ($GJRGA_S$)

algorithm (JRGA). One of the most important JRGA is self-affine Brownian algorithm (Kulatilake *et al.* 1998). Understanding the parameters of the Brownian algorithm is difficult. Therefore, in this study a new Geostatistical JRGA is presented (GJRGA algorithm). In this algorithm meaningful parameters are used for generating joint roughness profiles. These include the range and standard deviation of asperities height according to the concept of primary and secondary roughness. Trend of joint roughness profiles is not independent of spatial position of asperities. Using primary and secondary roughness is a good method for evaluation of joint roughness.

4.1 GJRGA method for generating secondary roughness ($GJRGA_S$)

In order to generate secondary roughness by $GJRGA_S$, at the first, the standard deviation of asperities height of secondary roughness for10 joint roughness profiles of Barton were determined. The calculation illustrates SD_H of secondary roughness varies from 0.02 to 0.12 mm. Therefore for profiles with a length of 100 mm, random height data was generated using the Monte-Carlo method. These data are located on a profile with interval distance equal to 0.25 mm, consequently 401 data were generated with one run of the $GJRGA_S$. Finally for a specific SD_H, joint roughness parameter includes: Z_2, Z_3, R_P and SD_A were calculated for each generated profiles. In order to be representative of calculated parameters at generated profiles, for each specific SD_H, the $GJRGA_S$ were run 1000 times and average of joint roughness parameters were calculated for evaluation of secondary roughness. Flowchart of $GJRGA_S$ is shown in Fig. 11. The GJRGA method for generating secondary roughness includes the following steps:

1- Determination of PDF of secondary asperities height (PDFs): subtraction of fourth-order polynomial equation from general profile is defined as residual value (e(x) =z(x)-m(x), Fig. 9). In this paper PDF of e(x) is defined PDFs.

2- Determination of distance of two random points (D_r) on the profile length (L). In this paper D_r were selected equal to 0.25 mm. Khanh *et al.* (2018), generated random profiles with 0.25 mm interval.

3- Generating random data, e(x), from the PDFs by Monte Carlo method, N_S at Eq. (3)

4- Determination of joint roughness parameters (such as Z_2, Z_3, R_p)

$$N_s = \frac{L}{D_r} + 1 \tag{3}$$

At each run of this algorithm for specific geostatitical parameters (D_r and SD_H) the SD_A was calculated. Running $GJRGA_S$ for specific range of geostatistical parameters leads to a geostatistical classification.

4.2 GJRGA method for generating primary roughness ($GJRGA_P$)

In order to generate the primary roughness by $GJRGA_P$, at the first, range and standard deviation of asperities height of primary roughness were determined for ten joint roughness profiles of Barton. The range of variation of SD_H and range is between 0.2 to 2 mm and 5 to 50 mm respectively. At determined limits were selected 10 different values of SD_H and range. Generally 100 different scenarios was evaluated. For each of these 100 scenarios, generated asperities height was located on a 100 mm length profile with interval distance equal to a specific range. For example, a scenario with a specific SD_H and a range equal to 10 mm, 11 asperities height generates by Mount-Carlo method and locates on a 100 mm profiles with interval distance equal to 10 mm. After generating a roughness profile a four-order polynomial equation is fit to the generated data. This equation is defined as a primary roughness. Finally for a specific range and SD_H, joint roughness parameter for primary roughness includes: Z_2, Z_3, R_P and SD_A was calculated for each generated profiles In order to be representative of calculated parameters at generated profiles, for each specific SD_H , the $GJRGA_P$ were run 1000 times and average of joint roughness parameters was calculated for evaluation of secondary roughness. Generally for evaluation of primary roughness the $GJRGA_P$ were run 100000 times.

The GJRGA method for generating primary roughness includes the following steps ($GJRGA_P$). Flowchart of GJRGAP is shown in Fig. 12.

1- Determination of PDF and range of asperities height

2- Determination of trend of Barton profiles as a fourth-order polynomial

3- Data generation from asperity height PDF by Monte Carlo method (m(x) in Fig. 9): where L is the profile length and “a” is the range. The number of generated data

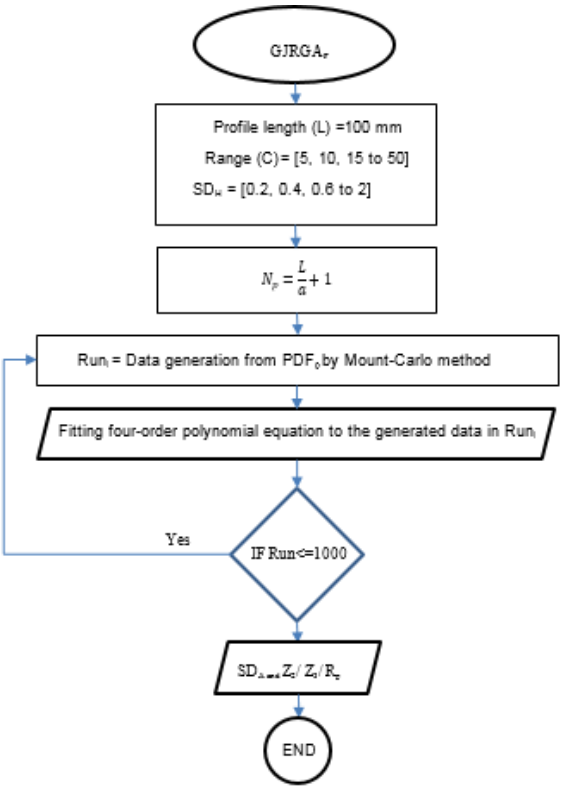

Fig. 12 Geostatistical joint roughness generation algorithm for primary roughness (GJRGA$_P$)

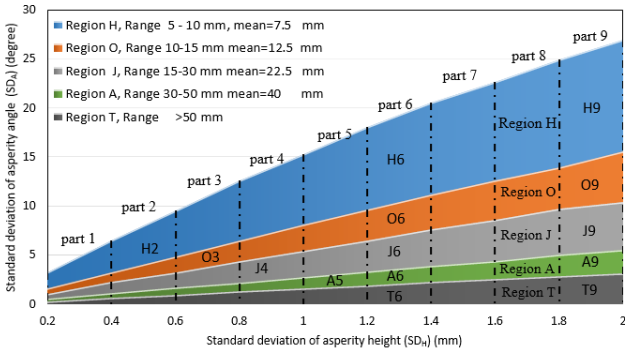

Fig. 13 Geostatistical classification of joint roughness for primary roughness (GCJR$_P$)

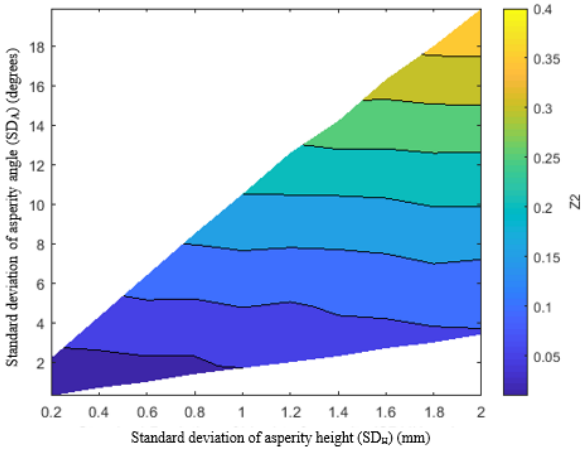

Fig. 14 The Geostatistical contour diagram of Z_2

was calculated from Eq. (4). Similar to standard profiles of Barton, 10 cm was considered for the profile length.

$$N_p = \frac{L}{a} + 1 \tag{4}$$

4- Fitting the fourth-order polynomial equation to the generated data: This polynomial is defined as the primary roughness.

5- Determination of joint roughness parameters (such as SD_A, Z_2, Z_3, R_p)

Considering SD_H and the range of asperities (Table 1) at the proposed algorithm the mean of SD_A was determined for different geostatistical parameters. At each run of this algorithm for a specific geostatitical parameters (range and SD_H) the SD_A is calculated. Running of GJRGA$_S$ for a range of geostatistical parameters leads to a geostatistical classification.

5. Geostatistical classification of joint roughness

The defined joint roughness parameters such as Z_2, Z_3, R_P do not change linearly by changing the JRC value (Tatone and Grasselli 2010). This means that Barton profiles have relatively an ordinal scale. No mathematical definition for standard joint roughness profile so far. According to the GJRGA$_P$, SD_A changes with a constant trend when the range is constant and SD_H changes. Hence, to achieve the constant variation of SD_A (constant slope) the proposed algorithm was run at each loop with a constant range and different SD_H. According to Table 4, the range and SD_H were changed between 5-50 mm and 0.2-2 mm respectively. The output of each loop of the algorithm is SD_A. Thus, for any initial state the algorithm was run 1000 times and the average of each state is reported as the result. The output of GJRGA$_P$ flowchart is illustrated in Fig. 13. This is geostatistical classification of joint roughness for primary roughness (GCJR$_P$). At a constant range, value of SD_A is changed linearly. The SD_A is a function of SD_H and range. This relation was defined by Eq. (5).

$$SD_A = \alpha.range^{\beta}.{SD_H}^{s} \tag{5}$$

where the value of s was considered equal to one for primary roughness. Reduction of the range leads to increasing the nonlinear relation between SD_H and SD_A. In this paper the value of α and β were calculated 68.497 and -0.948 respectively. The regions between two sequential curves of the GCJRp were named by H, O, J, A and T letters. Variations of ranges at the H, O, J, A regions are changed between 5-10, 10-15, 15-30 and 30-40 mm respectively. The Range at the region T is more than 50 mm. The average number of asperities at each region is constant. According to the proposed algorithm, the number of asperities has a direct relationship with the range of data. Each region is divided into the 9 parts. Variation of SD_H in each part is 0.2 mm. As SD_H increases, the height of the generated asperities increases and asperities become sharper. As can be recognized in Fig. 13, at a specific range (a specific curve) relation between SD_H and SD_A is linear.

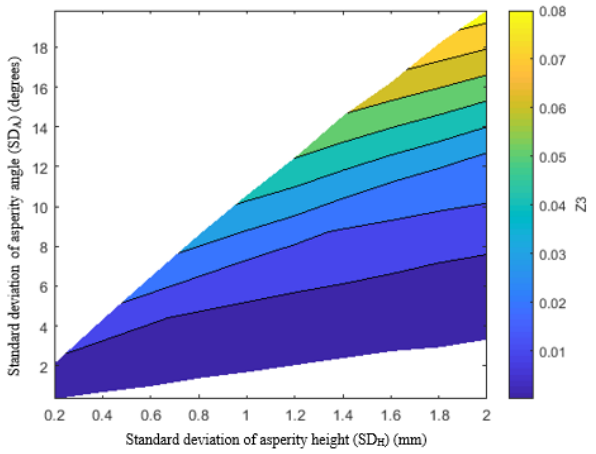

Fig. 15 The Geostatistical contour diagram of Z_3

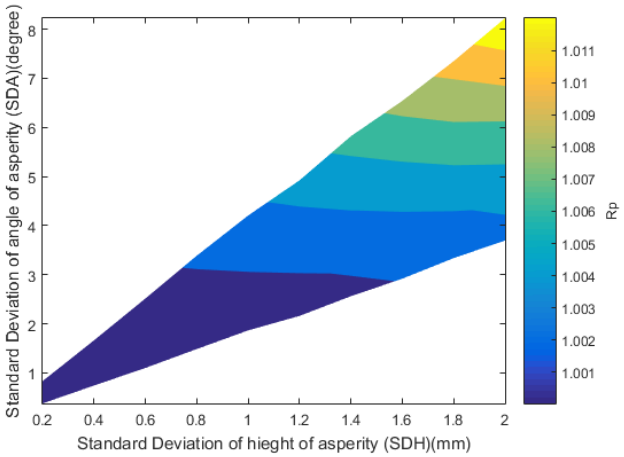

Fig. 16 The Geostatistical contour diagram of R_P

As the range in $GJRGA_P$ becomes larger (the base of the asperities) the shape of asperities becomes flatter. The results illustrate that joint profiles have larger SD_A with increase of SD_H and decrease of range.

The average number of asperities in each specific part is constant and with increasing the SD_H the ratio of height to base of the asperities (H/B ratio) increases and the asperities become sharper. On the other hand, at a specific part of SD_H (Ex. 1.8 to 2) the asperities become more elongated with decreasing the range. Asperities with high range and small SD_H showed a small H/B ratio and generated smoother profiles. On the other hand, asperities with low range and high SD_H are asperities with a high H/B ratio and hence the asperities become larger. Fig. 13 represents a conceptual classification for general shape of asperities. According to the proposed algorithm, the values of roughness parameters were calculated for each point in Fig. 13. The contour diagrams of Z_2, Z_3 and R_P parameters are shown in Figs. 14, 15 and 16 respectively.

The contour diagrams of Z_2 are approximately horizontal. This shows that asperities with high SD_H and low range have lower Z_2 (around the region H9). Asperities with different shapes at specific regions have the same Z_2. As mentioned above the number of asperities at region H is larger compared to regions O, J and A and increasing the

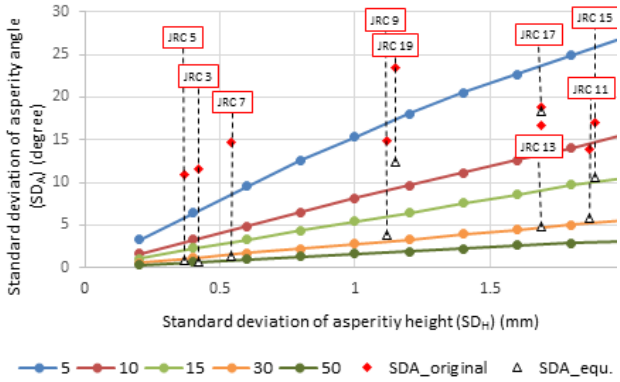

Fig. 17 SD_A as a function of SD_H for primary roughness at different range

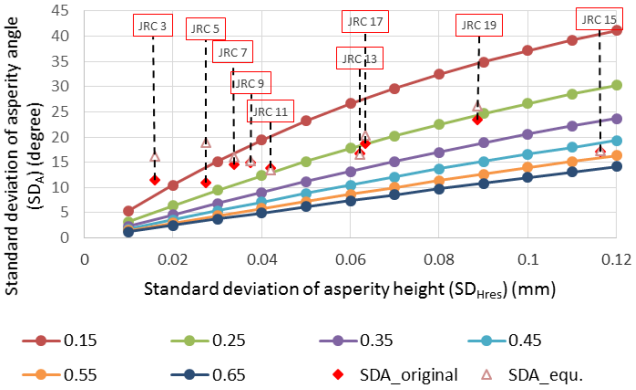

Fig. 18 SD_A as a function of SD_{Hres} for secondary roughness

number of asperities lead to large values of Z_3. Fig. 15 shows that as the number of asperities increases the value of Z_3 increases which corresponds to the definition of Z_3.

Variation of Z_3 vs. SD_H is more than that of Z_2 vs. SD_H Fig.16 illustrates contour diagram of R_P at different geostatitical parts and regions. As can be seen, the maximum value for R_P as similar as Z_2, Z_3. Large differences in the results like the existence of the same values of a parameters or different geostatistical conditions illustrate that the Z_2, Z_3 and R_P consider some part of the joint roughness description.

The contour diagrams is shown in Figs 14, 15 and 16 have not similar contour. It demonstrates that the statistical parameters have large discrete. Accordingly comparison of Figs 14, 15 and 16 display for a specific geostatistical parameter, joint roughness parameters (Z_2, Z_3, R_p and SD_A) have a different result which leads to estimation of different roughness.

6. Discussions

SD_A values for Barton profiles were calculated with Eq. 5, using the range and SD_H values from Table 1. The results are illustrated with triangles in Fig. 17. The SD_A of original Barton profiles were also calculated directly from the original Barton profiles ($SD_{Aoriginal}$) and are illustrated by circles in Fig. 17. In most cases, SD_A increases with increasing roughness. In some cases, such as JRC 3 and 5, the SD_A was decreased. The JRC 7, 9 and 11 have the same

SD_A approximately, but it is clear that the location of these profiles in Fig. 17 is different. This difference is due to the different shape of the asperities for these Barton profiles. The predicted value differs significantly from the actual value calculated directly from the Barton profiles. Therefore, the trend of asperities (general shape of the asperities, implemented in step 4 of the proposed algorithm) has little effect on the SD_A value.

In order to investigate the effect of secondary roughness, the trend of data was removed from Barton profiles (primary roughness was omitted) and the values of standard deviation of residuals (SD_{Hres}) were calculated. SD_{Hres} is changing between of 0.01 and 0.12 mm. The SD_A values of the secondary asperities were calculated at different intervals.

Fig. 18 shows the classification of secondary asperities for different geostatistical parameters. Similar to what was observed in Fig. 17, with increasing SD_{Hres} the SD_A for different intervals increases. SD_A values for original Barton profiles were calculated directly from the original Barton profiles ($SD_{Aorginal}$) as illustrated in Fig. 18 by the rhomb markers. SD_A of the roughness was calculated using Eq. (5). The values of α and β for the secondary roughness were calculated 89.318 and -0.716, respectively. The $SD_{Aoriginal}$ and the estimated values are very close. The results show that the secondary roughness has a great influence on the roughness values.

7. Conclusions

In this study, a geostatistical method for generation of two-dimensional joint roughness profiles over complex terrain has been proposed in this study. Evaluation of joint roughness profiles using geostatistical parameters showed:

• Changes of joint roughness are not independent of the range

• The SD_H and range of joint profiles have a great effect on joint roughness parameters.

• According to the range and SD_H, different geostatistical parts for primary and secondary roughness were classified.

• Parameters Z_2, Z_3 and R_p have different results at the same geostatistical parameters

• The secondary roughness has a great influence on roughness values

• The presented conceptual classification for the shape of the asperities can be used as a useful method for the description of joint roughness.

• In general, it can be concluded that examining the shape and size of the asperities is a good solution to move from the laboratory scale to the field scale.

Acknowledgments

This work has been supported by Kashigar Geo-mechanics Research Center (KGMC).

References

Asadi, M.S., Rasouli, V. and Barla, G. (2012), "A bonded particle model simulation of shear strength and asperity degradation for rough rock fractures", *Rock Mech. Rock Eng.*, **45**(5), 649-675. https://doi.org/10.1007/s00603-012-0231-4.

Atapour, H. and Moosavi, M. (2014), "The influence of shearing velocity on shear behavior of artificial joints", *Rock Mech. Rock Eng.*, **47**(5), 1745-1761. https://doi.org/10.1007/s00603-013-0481-9.

Babanouri, N. and Karimi-Nasab, S. (2015), "Modeling spatial structure of rock fracture surfaces before and after shear test: A method for estimating morphology of damaged zones", *Rock Mech. Rock Eng.*, **48**(3), 1051-1065. https://doi.org/10.1007/s00603-014-0622-9.

Babanouri, N., Nasab, S.K. and Sarafrazi, S. (2013), "A hybrid particle swarm optimization and multi-layer perceptron algorithm for bivariate fractal analysis of rock fractures roughness", *Int. J. Rock Mech. Min. Sci.*, **60**, 66-74. https://doi.org/10.1016/j.ijrmms.2012.12.028.

Barton, N. and Choubey, V. (1977), "The shear strength of rock joints in theory and practice", *Rock Mech.*, **10**(1-2), 1-54. https://doi.org/10.1007/BF01261801.

Chen, S.J., Zhu, W.C., Yu, Q.L. and Liu, X.G. (2016), "Characterization of anisotropy of joint surface roughness and aperture by variogram approach based on digital image processing technique", *Rock Mech. Rock Eng.*, **49**(3), 855-876. https://doi.org/10.1007/s00603-015-0795-x.

Fathi, A., Moradian, Z., Rivard, P., Ballivy, G. and Boyd, A.J. (2016), "Geometric effect of asperities on shear mechanism of rock joints", *Rock Mech. Rock Eng.*, **49**(3), 801-820. https://doi.org/10.1007/s00603-015-0799-6.

Fecker, E. (1978), "Geotechnical description and classificatioin of joint surfaces", *B. Int. Assoc. Eng. Geol.*, **18**(1), 111-120. https://doi.org/10.1007/BF02635356.

Grasselli, G. (2001), "Shear strength of rock joints based on quantified surface description", Ph.D. Thesis, Swiss Federal Institute of Technology Lausanne, Lausanne, Switzerland.

Grasselli, G. and P. Egger (2003), "Constitutive law for the shear strength of rock joints based on three-dimensional surface parameters", *Int. J. Rock Mech. Min. Sci.*, **40**(1), 25-40. https://doi.org/10.1016/S1365-1609(02)00101-6.

Gravanis, E. and Pantelidis, L. (2019), "Determining of the joint roughness coefficient (JRC) of rock discontinuities based on the theory of random fields", *Geosciences*, **9**(7), 295. https://doi.org/10.3390/geosciences9070295.

He, Z.M., Xiong, Z.Y., Hu, Q.G. and Yang, M. (2014), "Analytical and numerical solutions for shear mechanical behaviors of structural plane", *J. Central South Univ.*, **21**(7), 2944-2949. https://doi.org/10.1007/s11771-014-2261-4.

Huan, J.Y., He, M.M., Zhang, Z.Q. and Li, N. (2019), "A new method to estimate the joint roughness coefficient by back calculation of shear strength", *Adv. Civ. Eng.* https://doi.org/10.1155/2019/7897529.

Kulatilake, P.H.S.W., Um, J. and Pan, G. (1998), "Requirements for accurate quantification of self-affine roughness using the variogram method", *Int. J. Solids Struct.* **35**(31-32), 4167-4189. https://doi.org/10.1016/S0020-7683(97)00308-9.

Lê, H.K., Huang, W.C., Liao, M.C. and Weng, M.C. (2018), "Spatial characteristics of rock joint profile roughness and mechanical behavior of a randomly generated rock joint", *Eng. Geol.*, **245**, 97-105. https://doi.org/10.1016/j.enggeo.2018.06.017.

Lotfi, M. and Tokhmechi, B. (2019), "Fractal-wavelet-fusion-based re-ranking of joint roughness coefficients", *J. Min. Environ.*, **10**(4), 1121-1133. https://doi.org/10.22044/JME.2019.7489.1614.

Matheron, G. (1963), "Principles of geostatistics", *Econ. Geol.*, **58**(8), 1246-1266. https://doi.org/10.2113/gsecongeo.58.8.1246.

Mechanics, I.S.F.R. (1978), *Suggested Methods for the Quantitative Description of Discontinuities in Rock Masses*,

Pergamon Press.
Park, J.W., Lee, Y.K., Song, J.J. and Choi, B.H. (2013), "A constitutive model for shear behavior of rock joints based on three-dimensional quantification of joint roughness", *Rock Mech. Rock Eng.,* **46**(6), 1513-1537. https://doi.org/10.1007/s00603-012-0365-4.
Rasouli, V. and Harrison, J. (2010), "Assessment of rock fracture surface roughness using Riemannian statistics of linear profiles", *Int. J. Rock Mech. Min. Sci*., **47**(6), 940-948. https://doi.org/10.1016/j.ijrmms.2010.05.013.
Tatone, B.S. and Grasselli, G. (2010), "A new 2D discontinuity roughness parameter and its correlation with JRC", *Int. J. Rock Mech. Min. Sci*., **47**(8), 1391-1400. https://doi.org/10.1016/j.ijrmms.2010.06.006.
Walck, C. (1996), *Hand-book on Statistical Distributions for Experimentalists*.
Wang, M., Chen, Y.F., Ma, G.W., Zhou, J.Q. and Zhou, C.B. (2016), "Influence of surface roughness on nonlinear flow behaviors in 3D self-affine rough fractures: Lattice Boltzmann simulations", *Adv. Water Resour*., **96**, 373-388. https://doi.org/10.1016/j.advwatres.2016.08.006.
Wittke, W. (2014), *Rock Mechanics based on an Anisotropic Jointed Rock Model (AJRM)*, John Wiley & Sons.
Yong, R., Gu, L., Ye, J., Du, S.G., Huang, M., Hu, G. and Liu, J. (2019), "Neutrosophic function with nns for analyzing and expressing anisotropy characteristic and scale effect of joint surface roughness", *Math. Prob. Eng*. https://doi.org/10.1155/2019/8718936.
Zhao, L., Zhang, S., Huang, D., Zuo, S. and Li, D. (2018), "Quantitative characterization of joint roughness based on semivariogram parameters", *Int. J. Rock Mech. Min. Sci*., **109**, 1-8. https://doi.org/10.1016/j.ijrmms.2018.06.008.

GC